Supporting Information

Enabling in-situ studies of Metal-Organic Chemical Vapor Deposition in a Transmission Electron Microscope

Marcus Tornberg, Carina B. Maliakkal, Daniel Jacobsson, Reine Wallenberg, and Kimberly A. Dick

Centre for Analysis and Synthesis, Lund University, Box 124, 22100, Lund, Sweden

National Center for High Resolution Electron Microscopy (nCHREM), Lund University, 22100, Lund, Sweden

and

NanoLund, Lund University, 22100, Lund, Sweden

SI-1: DESIGN OF INSTRUMENTATION - MICROSCOPE ILLUSTRATION

Figure S1 illustrates the Hitachi 3300S instrument which is installed to facilitate semiconductor growth within the objective pole-piece gap. The microscope is equipped with a 300 keV cold field emission gun and and spherical aberration corrector (CEOS B-COR) for the objective lens. Specifically, the illustration shows the location of the intermediate chamber created and the additional ion pump (III) that assists the differential pumping above the sample. In addition, it shows how the gas-handling system is connected to the microscope at the sample region, which is done either through the holder or through a side-port injector. The pressure in the microscope is measured by one of the two magnetron pirani (pressure) gauges (Inficon MPG400) located within the column, by the objective pole piece, or towards the turbo pump operating on the objective pole-piece gap. To further probe the ambient leading away from the sample, the latter pressure gauge is supported by a residual gas analyser (SRS RGA300amu). Holders for the gas delivery allow joule heating, parallel gas delivery through the holder and rotation of the holder along its axis. In the case of delivering gases directly to the objective pole-piece gap, the holder is designed to accommodate both joule heating and rotation along both axes of the sample. The main text is mainly focusing on imaging and analysis using EDS, pressure control and the recording on the Gatan OneView IS camera.

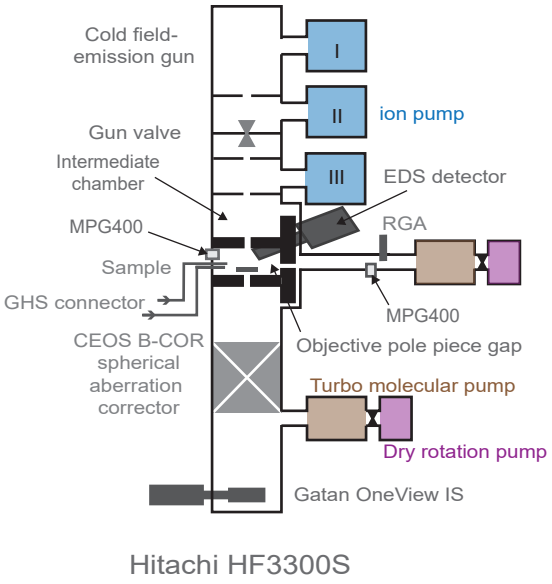

FIG. S1. A simplified schematic of the environmental transmission electron microscope.

SI-2: MICROSCOPE ENVIRONMENT

The state of the ambient at the sample is monitored by observing the pressures in the microscope column (P_{Col}) and just prior the connection between microscope and gas-handling-system (P_{Line}). Figure S2 shows how the pressure before and after the sample responds to increases and decreases change in mass flow (here: AsH_3). From calibrations in the main text, the sample pressure is related to the column pressure by a factor of approximately 2 (depending on sample orientation). The pressure that is measured on the high-pressure side of the GHS-Microscope connection, is here 200 times higher due to differential pumping through the capillary tubing, a differential pressure which depends on the length of the capillary as stated in the main text. The time needed for both these pressures reach a time-invariant state, are the measure of our system's response time to gas changes. Note that decreases in flow do respond more rapidly in comparison to increases of the gas flow.

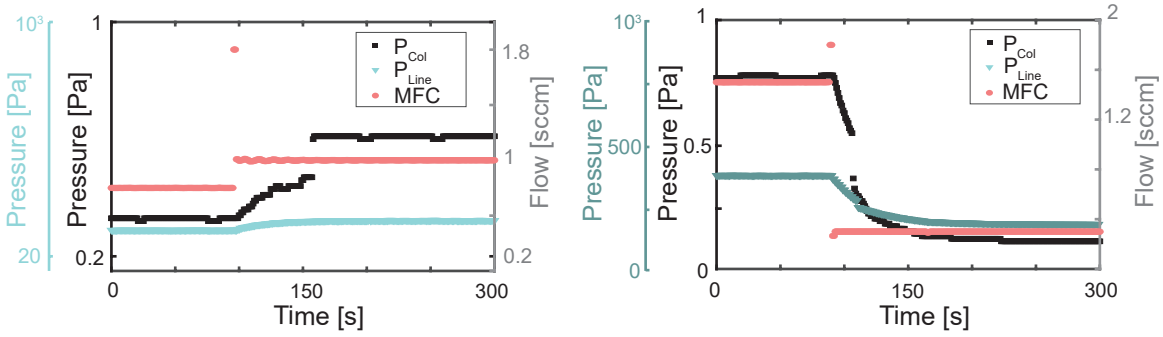

FIG. S2. The response time of the system for reaching a new higher, and lower gas flow set point. We see that the column pressure and the gas line pressure responds readily to changes in mass flow and stabilizes within 100 s to a new ambient equilibrium. Presented data is acquired when supplying gas through a column side port, directly to the pole-piece gap

The partial pressures in the gas evacuated towards the turbo molecular pump are measured by residual gas analyzer has shown interdependence of gas species. Here we showcase the fact that the precursor derivates of TMGa does change with increased AsH_3 supply. The interdependence is not necessarily monotone as in the case presented in Figure S3. However, for this specific material combination, supplying AsH_3 at 1 sccm provides the same response of TMGa derivatives as not supplying any AsH_3. This makes that particular flow especially useful for sweeping the TMGa concentration and still get a reliable quantification from the

RGA. The origin of this interdependence on partial pressures during RGA has yet to be evaluated but the observation is nevertheless necessary too provide a reliable probing of the environment during experiments involving more than one species.

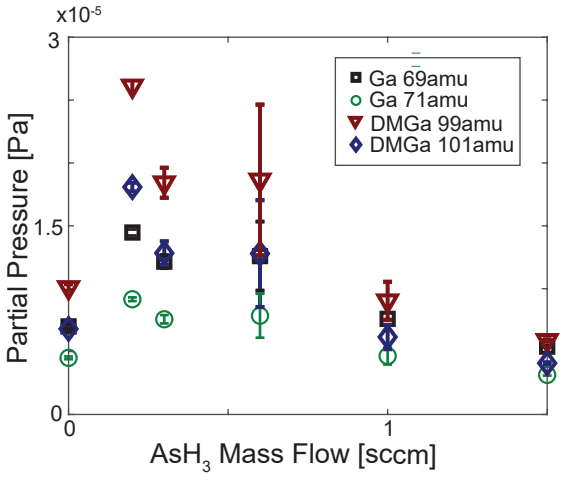

FIG. S3. Interdependence on residual gas analysis of AsH_3 on the partial pressure read-out of TMGa-derivatives for constant supply of TMGa (4.8e-5 mmol/min).

SI-3: TILT-DEPENDENT SAMPLE PRESSURE

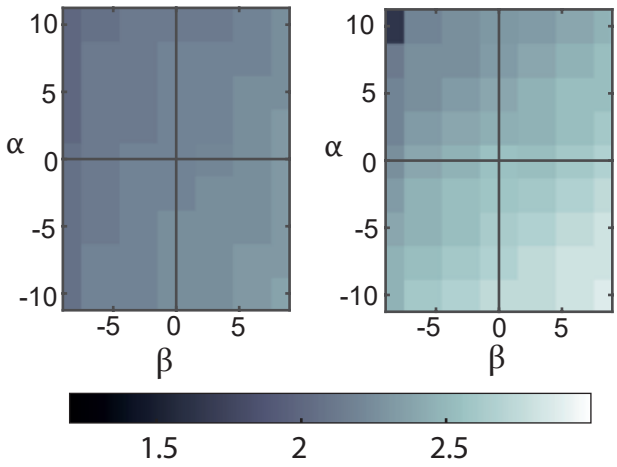

FIG. S4. Stage tilt-dependent calibration factors correlating the sample pressure of N_2 with respect to the column pressure which is obtainable during experiments for gas-injectors dedicated to group III (left) and group V (right) elements. The resulting colormap from the discrete measurements at intervals of 2.5° (α) and 3° (β) starting from the origin (0,0). The heatmaps shows the same information as Figure 3 in the main article, but for transparency these heat maps shows the measured data without data interpolation.

SI-4: IMAGING AND ANALYSIS OF A SAMPLE IN A REACTIVE ENVIRONMENT

Spatial Resolution

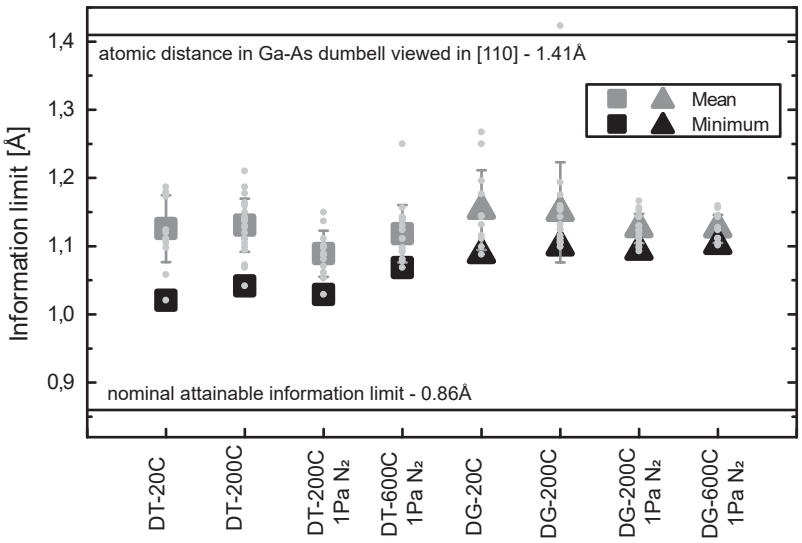

FIG. S5. The figure shows the detailed data behind the table of figure 5 in main article. It shows each individual measurement as dots as well as the collective mean (gray square) and best achieved information limit (black square). It is presented for the holder configurations that supply gas through the holder (DG) and through the sideport (DT). For each configuration, we present the information limit at 20, 200 and 600 °C as well as when increasing the background pressure of the microscope with 0 or 1 Pa of N_2. For reference, we introduced the minimum required information limit for atomically resolved imaging of GaAs (1.41 Å) as well as the nominal attainable information limit of the instrument using a standard Cu-C-grid at low pressure and room temperature (0.86 Å).

The resolution tests presented in the paper was performed in sequence using at least 6 images (minimum of 3 for each projection shift) of each environment configuration; at low mid and high temperature, and in vacuum and 1 Pa background pressure. The data set was then analyzed using Digital Micrograph (GMS3) by two individual operators and the result is presented for each holder and configuration in Figure S5. For transparency, all data is displayed as gray dots, while the mean and minimum information limit is represented by gray and black squares, respectively. From the dataset, we do not observe a large influence on the information limit for increasing pressure and temperature. However, the resolution

appears to be influenced by the holder type. The two holder designs are labeled as Double Tilt (DT) and Double Gas (DG) as it is the main feature of the holders. Remember that the DT-holder also gets two gases to the sample, however, not through the holder itself but through the microscope sideport. Both holders are used for the purpose of environmental TEM and are designed by Hitachi High-Tech Canada. For perspective on the resolution, the two lines in Figure S5 represents the specified and attainable information limit of the microscope on a standard holder in normal operation (0.86 Å) and the relevant interplanar distance of a typical III-V semiconductor (here GaAs [1 1 0]).

Influence of elevated pressure on the beam current

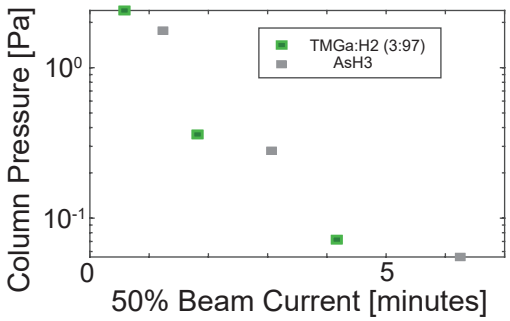

FIG. S6. Time until the cold-FEG reaches 50% of its set emission (from 10 µA to 5 µA) with respect to the corrected pressure of AsH_3 and TMGa:H_2 in the column.

The fact that we have an open system with an installed cold-FEG leads to a faster decrease in emission for the electron gun. This in turn requires more frequent in-operation flashing of the FEG, even when supported by an additional ion pump, to keep a good image quality. Figure S6 shows the extreme cases where we supplied high flows of precursor material to the microscope and investigated how long time the gun valve can be open before the beam current has been reduced to half of its set point (from 10 µA to 5 µA). The figure shows that a background pressure of 1 Pa of either AsH_3 or TMGA:H_2 mixture allows less than a couple of minutes for imaging at with the high dose. While this is pushing the limits of the for the column pressure of the instrument it is still possible to perform imaging and analysis beyond this point but at the cost of a lower electron dose. This is not necessarily a drawback unless the analysis you are making is highly sensitive to time or intensity. In

addition, this type of limitation and information serve as useful information when exploring instrument design and optimization for specific reaction experiments.

SI-5: TEMPERATURE EFFECT ON X-RAY ENERGY-DISPERSIVE SPECTROSCOPY

As a result the increased shift with elevated temperature and dead-time we investigated the intensity as a function of temperature. To obtain a reliable spectra at temperatures beyond 600 °C on SiN_x membrane MEMS we retracted the detector to reduce the solid angle and thus the intensity and the corresponding dead-time of the detection process. The result shows in figure S7 a clear trend between the energy shift of the strobe-peak and the dead-time/intensity. When observing elemental peaks such as the Si K_α we notice a similar shift in energy albeit smaller.

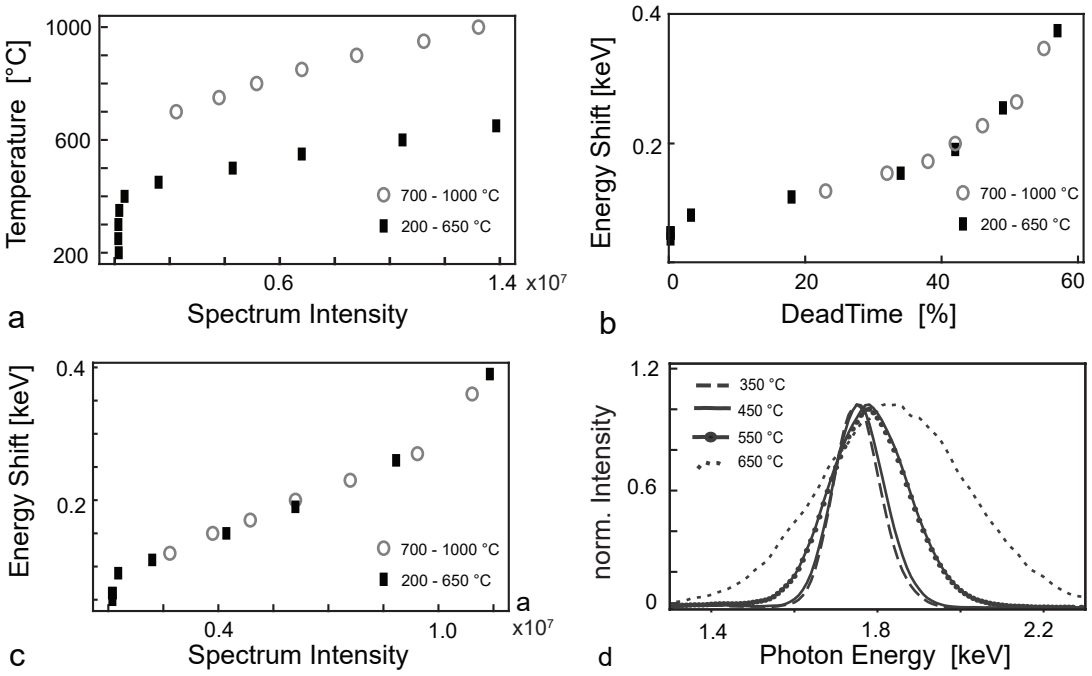

FIG. S7. How temperature influences the detected intensity and in turn the elemental peaks within the energy dispersive spectra. (a) shows how reducing the solid angle effects the total intensity of the acquired spectra and (b,c) shows how this translates in shift of the strobe-peak. The dataset from a smaller solid angle is presented as circles while the standard solid angle collection is represented by squares.(d) shows how the elemental peak of Si at 1.74 keV shifts its peak position as a result of the increased temperature, visualizing the magnitude of the effect.